SAND2008-0540C

Imaging Oxide-Covered Doped Silicon Structures Using Low-Energy Electron Microscopy

M.L. Anderson, C.Y. Nakakura, K.F. Saiz, and G.L. Kellogg
Sandia National Laboratories, Albuquerque, NM, 87123

ABSTRACT

Low energy electron microscopy (LEEM) operated at incident electron energies just above the "mirror" mode is used to image Si-based test devices. Significant *p*- vs. *n*- doping contrast is observed, even when the structures are covered with a ~3.5 nm thermal oxide. The contrast arises from a difference in surface potential between the two regions and is related to both *p*-*n* work function differences and electron-beam-induced charging of the oxide. The results show that the LEEM is capable of characterizing *pn* junctions without complicated sample preparation and that it is a promising technique for rapid, non-destructive imaging of microelectronic devices.

INTRODUCTION

With the continuing decrease in microelectronic feature sizes, and resulting increase in complexity of IC's, there is a strong incentive to develop device imaging techniques that offer both high spatial resolution and high sample throughput. The low energy electron microscope (LEEM), with a spatial resolution of 7-8 nm, a parallel imaging scheme and multiple contrast mechanisms is potentially such an instrument. Although the related technique of photoemission electron microscopy (PEEM) has been used successfully to image doping variations in various device structures [1-6], comparatively little work has been reported to assess the capabilities of the LEEM. Here, we report a LEEM investigation to image *pn* test structures buried under a ~3.5 nm thermal oxide. We find surprisingly good contrast between doping type when imaging with electron energies of just a few volts above the mirror mode (electron reflection). We also observe time-dependent changes in the image intensity indicating significant electron beam charging of the oxide during the measurements. The charge on the oxide persists for periods of hours to days and has a marked effect on the optimum electron energy used for imaging.

EXPERIMENT

The experiments detailed in this paper were performed using a commercial LEEM [7]. In this type of microscope, high-energy electrons (20 kV) from an electron gun (a LaB_6 source in our system) are focused on the back focal plane of an objective lens producing a parallel beam at the sample surface. Low electron energies at the sample are achieved by biasing it at a negative potential near to that of the source. The difference between the source and sample potential is called the start voltage, V_s. Depending on the value of V_s (-2 to +3 V in this study), electrons are either reflected (mirror electron microscopy, MEM) or scattered (LEEM) from the surface. The image formed by the objective lens using these electrons are re-accelerated to 20 kV, transferred by a magnetic prism, magnified by a series of lenses and projected on to a viewing screen.

Figure 1 shows a plot of how the reflected or scattered electron intensity varies as a function of V_s at low electron energies. When the sample potential is more negative than the gun potential (MEM), electrons are reflected before hitting the surface and the intensity is at its maximum. When the start voltage exceeds an onset potential (V_{onset}), electrons flow and the reflected electron intensity goes down. The onset occurs when the vacuum energy levels of the gun and sample align, so the onset voltage is given by the difference in work function between the sample and electron gun. As the start voltage is further increased, the intensity becomes higher due to the increase in backscattered electrons as a function of electron energy. We refer to these plots of intensity as a function of start voltage as "reflectivity curves." The range of start voltages where these changes in intensity occur is typically from -3 V to 5 V. When there are two regions on a surface with different work functions, the onset voltage occurs at different voltages. As shown below, by choosing the appropriate start voltage for imaging, there can be significant contrast based on the work function difference between the two regions.

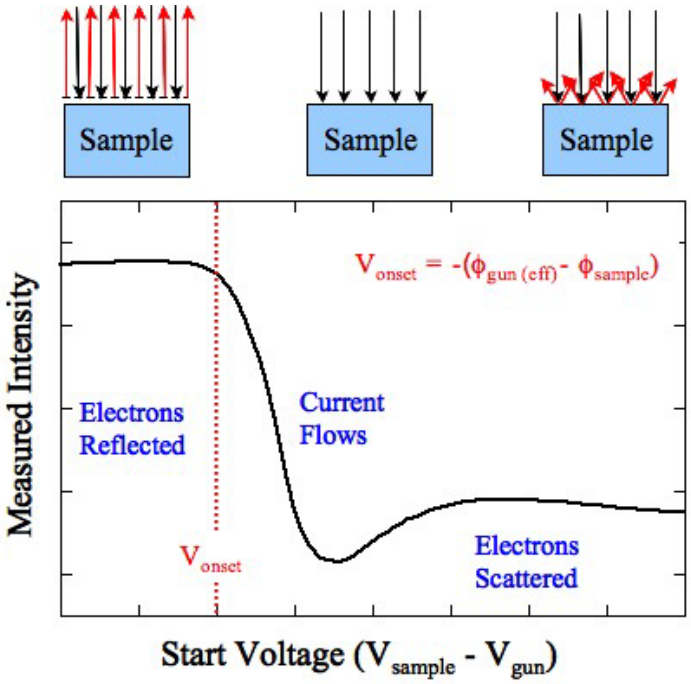

Figure 1. A reflectivity curve showing the general behavior of the measured intensity as a function of increasing start voltage when changing from the MEM to LEEM imaging modes.

The diode test structures used in this study were fabricated at Sandia National Laboratories MESA facility. Arsenic (As) and/or boron (B) were implanted into Si(100) *p*-type substrates to construct n^+/p junctions. Figure 2 shows cross-sectional (a) and top-down (b) schematics of the structures. A thermal oxide of ~ 3.5 nm thickness is indicated in (a). The regions of *n* vs. *p* doping are shown in (b). The doping concentration of the *n*-type region (blue) is ~10^{17} cm^{-3}. A series of *n*-type lines ranging in width from 0.25 μm to 1.1 μm extend into the *p*-type region (red) with a concentration of ~10^{19} cm^{-3}. The black circles on (b) indicate two locations where LEEM images (shown below) were acquired. Sample preparation consisted of sonicating the test structures in isopropyl alcohol.

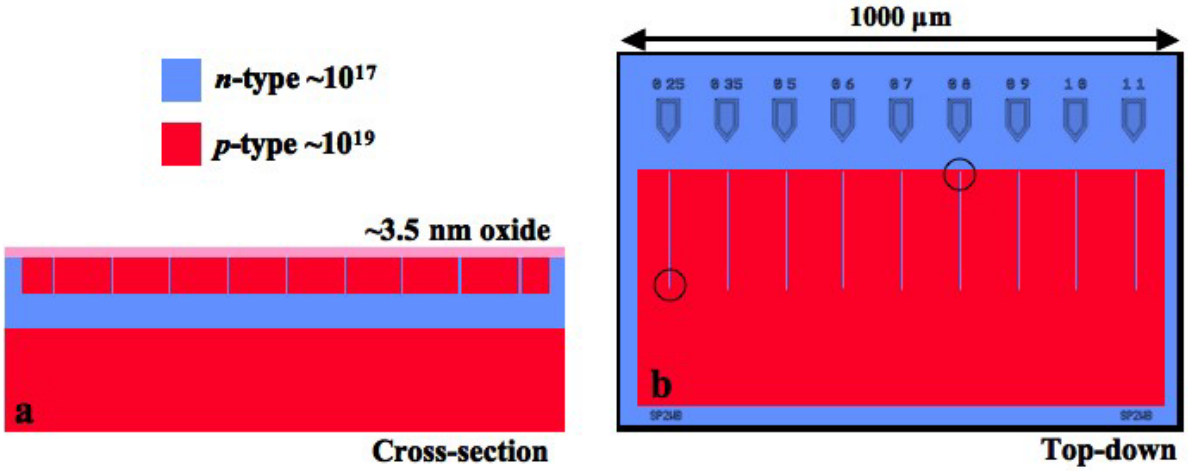

Figure 2. (a) Cross-sectional and (b) top-down schematics of test structures imaged with LEEM.

RESULTS AND DISCUSSION

Figure 3 shows 20 µm field-of-view LEEM images of the *n*-type lines (widths of 0.25 µm, 0.5 µm, and 0.8 µm). The position of the acquired image in Figure 3(a) is indicated by the bottom left circle in Figure 2(b). The *p*-type region appears bright and the *n*-type lines appear dark at a start voltage of 1.0 V. The widths of the lines determined from the images are found to vary with imaging conditions, but are typically within 20% of the doping line widths. Given the presence of the thermal oxide on the surface and the minimal sample preparation procedures, the observation of *p*-*n* contrast in the LEEM was quite unexpected.

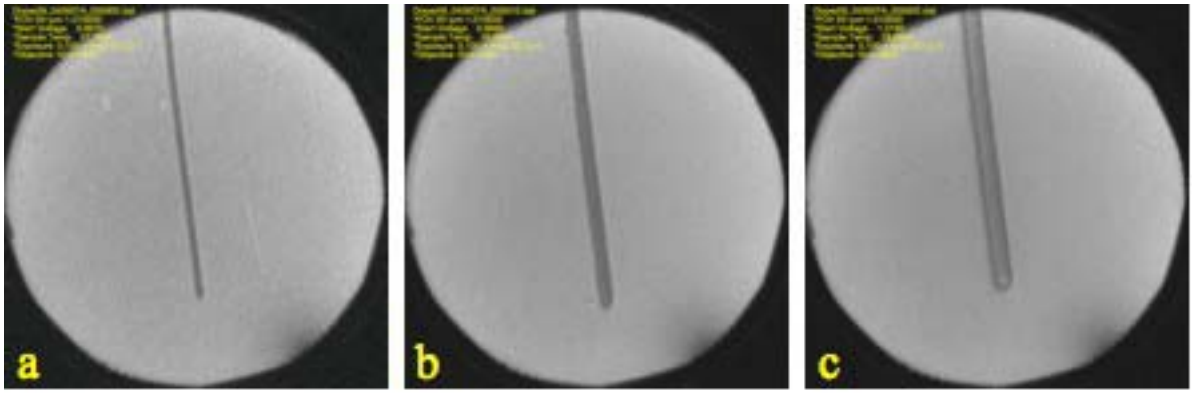

Figure 3. LEEM images of *n*-type lines a) 0.25 µm, b) 0.5 µm, and c) 0.8 µm, with *p*-type background, 20 µm field of view.

Figure 4 shows how the *p*-*n* contrast varies as a function of start voltage. Three images of the 0.5 µm line are shown at start voltages of -2.00 V, -0.15 V, and 0.70 V. It is clear from the figure that the contrast reverses when increasing the start voltage from -0.15 V to 0.70 V. This reversal is understood in terms of the reflectivity curves from the *n*- and *p*-type regions shown in Figure 5. With V_s = -2.0 V (Figure 4a) both the *n*- and *p*-type regions are bright. This corresponds to the MEM mode where electrons are reflected and the intensity is at its maximum

for both the *n*- and *p*-type regions. When V_s = -0.15 V (Figure 4b), the *n*-type region is dark and *p*-type region is bright. This voltage is above the onset voltage for current flow for the *n*-type region, but below that for the *p*-type region. Electrons are reflected from the *p*-type region (bright) but there is current flowing in the *n*-type region (dark). In (c), with V_s = 0.7 V, the intensity from the *n*-type region is higher because the number of backscattered electrons has increased. The intensity of the *p*-type region is lower because the onset voltage this region has been exceeded. The fact that V_{onset} occurs at a more negative voltage for the *n*-type area in Figure 5 is expected since the work function of *n*-type Si is smaller than for *p*-type. However, the separation between the reflectivity curves (1.5 V) is significantly larger than the work function difference between *n*- and *p*-type Si (0.7 eV). An additional effect is needed to account for the increased separation between the curves.

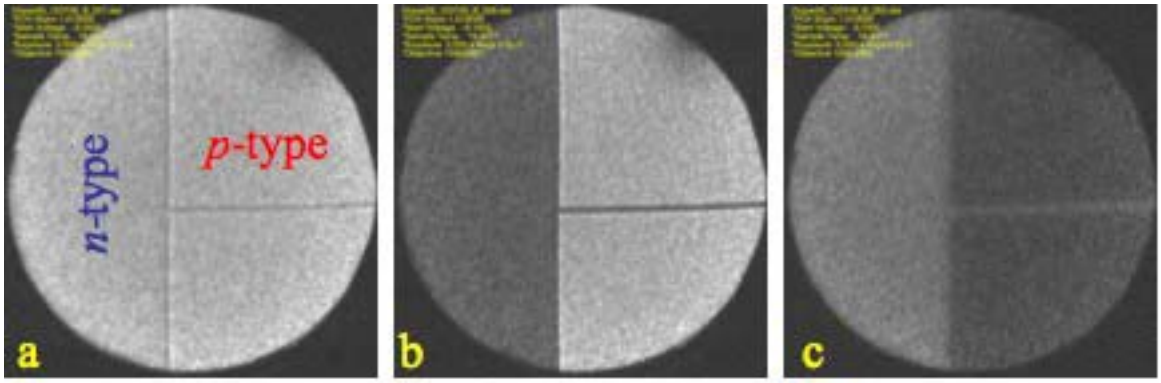

Figure 4. LEEM images of 0.5 μm *n*-type line at start voltages of a) -2.0 V, b) -0.15 V, and c) 0.7 V, 50 μm field of view.

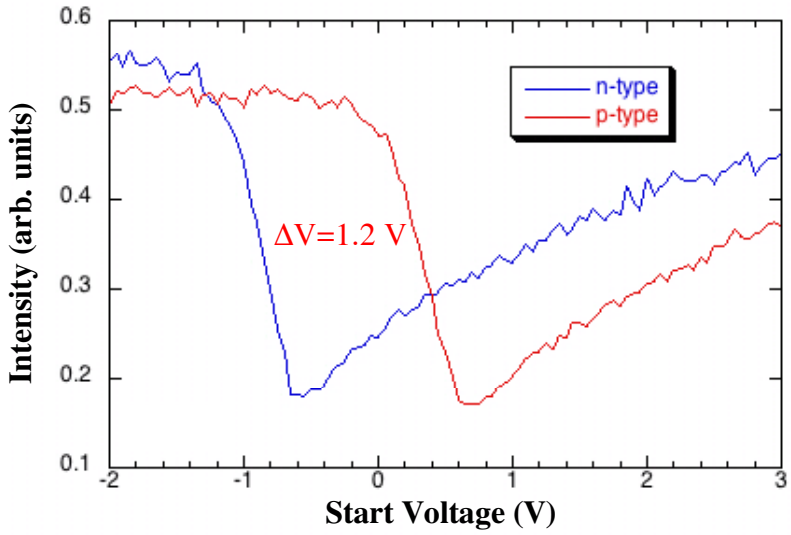

Figure 5. Reflectivity curves for *n*- and *p*-type Si regions of test structures.

The additional effect impacting the onset voltage of the reflectivity curves in our experiments is electron-beam-induced charging of the thermal oxide. Clear evidence for charging is seen in Figure 6. The images are individual frames taken from a video sequence during which the sample is translated under the beam. The start voltage in all three images is 0.0 V. Image (a) is

recorded after allowing the intensity to stabilize for several minutes. The sample is translated in a vertical direction to a new region just before recording image (b). The curved line separating the light and dark contrast in the *p*-type region is the edge of the beam spot. The freshly exposed *p*-type region is momentarily dark and then proceeds to get bright as a function of time. The increase in intensity is caused by a time-dependent change in surface potential. As the oxide becomes more negatively charged, the imaging mode changes from LEEM back to MEM. Eventually, the new region (c) is charged to the same potential as the initial image (a). Two points worth noting are that (1) the charged region is highly localized, as evidenced by the sharp line dividing the charged and uncharged region in (b), and (2) the charge persists for hours to days. For example, samples left overnight are still charged when imaged the next day. However, we find the regions can be "discharged" by increasing the electron energy to higher positive values (tens of volts). Here, the backscattered current exceeds the incident current and the oxide charges positively. Figure 6 also shows that the oxide above the *p*-type region has a more pronounced sensitivity to electron beam charging than that above the *n*-type region. This sensitivity, however, depends on the start voltage. When the start voltage is held at 0.0 V, as in Figure 6, the *p*-type region shows the strong time-dependent behavior. At more negative values of V_s, the intensity from the *n*-type region changes more strongly with time.

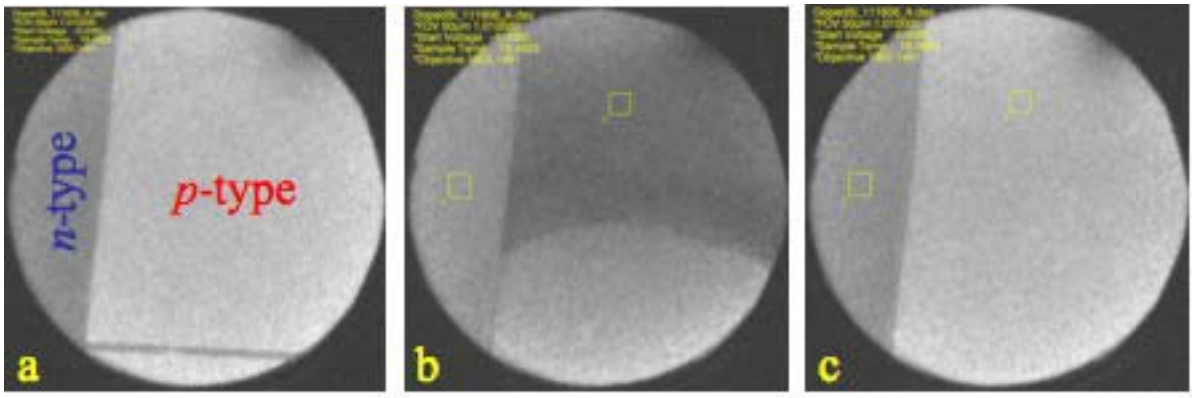

Figure 6. LEEM images showing the effect of oxide charging, start voltage = 0 V, 50 μm field of view.

The above results show that charging of the oxide by the imaging electron beam affects the surface potential that, in turn, determines the ratio of scattered to reflected electrons. This complicates the interpretation of reflectivity curves such as the ones in Figure 5. The difference in onset voltage is not simply the difference in work function between the two regions, but includes the difference in surface potential due to charging. This is important because the charging can depend on factors other than the *n* vs. *p* doping difference. For example, from atomic force microscope (AFM) images, we know that the thickness of the oxide above the two regions is not the same. The doping concentrations are also markedly different. So, is the contrast due to differences in *n* vs. *p* doping, difference in oxide thickness, or differences in doping concentrations? To address this question, we are examining samples with varying oxide thickness and varying dopant concentrations. The results, which will be published elsewhere [8], show that the onset voltage and thus the contrast mechanism depends on all three.

CONCLUSIONS

In summary, we have shown that LEEM can be used to image doped Si test structures buried under ~3.5 nm thermal oxides. The reflected/scattered electron intensity from the *n*- and *p*-type regions first decreases rapidly and then increases as a function of increasing start voltage (the sample bias relative to the electron gun bias). The start voltage at which the intensity begins to decrease (the change from MEM to LEEM imaging modes) is shifted in voltage for regions above the two types of doping. Thus, strong contrast can be achieved by "tuning" the start voltage. We also measure time-dependent oxide charging effects that are a function of both the start voltage and buried dopant type. Detailed mesurements to determine the relative contributions of dopant type, oxide thickness, and dopant concentration to the contrast mechanism are in progress [8].

ACKNOWLEDGMENTS

Sandia is a multiprogram laboratory operated by Sandia Corporation, a Lockheed Martin Company for the United States Department of Energy's National Nuclear Security Administration under contract DE-AC04-94AL85000.

REFERENCES

1. M. Giesen, R. J. Phaneuf, E. D. Williams, and T. L. Einstein, Surface Sci. **396**, 411 (1998).
2. V. W. Ballarotto, K. Siegrist, R. J. Phaneuf, E. D. Williams, and S. Mogren, Surface Sci. **461**, L570 (2000).
3. V. W. Ballarotto, K. Siegrist, R. J. Phaneuf, E. D. Williams, W.-C. Wang, and R. J. Nemanich, Appl. Phys. Lett. **78**, 3547 (2001).
4. V. W. Ballarotto, M. Breban, K. Siegrist, R. J. Phaneuf, and E. D. Williams, J. Vac. Sci. Technol. B, **20,** 2514 (2002).
5. K. Siegrist, V. W. Ballarotto, M. Breban, R. Yongsunthon, and E. D. Williams, Appl. Phys. Lett. **84**, 1419 (2004).
6. L. Frank, I. Müllerová, D. A. Valdaitsev, A. Gloskovskii, S. A. Neoijko, H.-J. Elmers, and G. Shönhense, J. Appl. Phys. **100**, 093712 (2006).
7. Elmitec Elektronnenmikroskopie, GmbH. For a review of the technique, see: E. Bauer, Rep. Prog. Phys. **57**, 895 (1994).
8. M. L. Anderson, C. Y. Nakakura, and G. L. Kellogg, unpublished.